



Original article

Surface plasma treatment effects on the molecular structure at polyimide/air and buried polyimide/epoxy interfaces



John N. Myers, Zhan Chen *

Department of Chemistry, University of Michigan, Ann Arbor, MI 48109, USA

ARTICLE INFO

Article history:

Received 4 November 2014

Received in revised form 22 December 2014

Accepted 25 December 2014

Available online 21 January 2015

Keywords:

Molecular structure

Vibrational spectroscopy

Sum frequency generation spectroscopy

ABSTRACT

Polyimides are widely used as chip passivation layers and organic substrates in microelectronic packaging. Plasma treatment has been used to enhance the interfacial properties of polyimides, but its molecular mechanism is not clear. In this research, the effects of polyimide surface plasma treatment on the molecular structures at corresponding polyimide/air and buried polyimide/epoxy interfaces were investigated *in situ* using sum frequency generation (SFG) vibrational spectroscopy. SFG results show that the polyimide backbone molecular structure was different at polyimide/air and polyimide/epoxy interfaces before and after plasma treatment. The different molecular structures at each interface indicate that structural reordering of the polyimide backbone occurred as a result of plasma treatment and contact with the epoxy adhesive. Furthermore, quantitative orientation analysis indicated that plasma treatment of polyimide surfaces altered the twist angle of the polyimide backbone at corresponding buried polyimide/epoxy interfaces. These SFG results indicate that plasma treatment of polymer surfaces can alter the molecular structure at corresponding polymer/air and buried polymer interfaces.

© 2015 Zhan Chen. Published by Elsevier B.V. on behalf of Chinese Chemical Society and Institute of Materia Medica, Chinese Academy of Medical Sciences. All rights reserved.

1. Introduction

Durable adhesion at the interface between polymeric adhesives and microelectronic package components is important for long-term package reliability [1]. Poor adhesion between epoxy adhesives and the chip passivation or organic substrate in flip chip packages can result in package failure caused by interfacial delamination at the adhesive interface during accelerated stress testing [2]. In particular, poor adhesion between polyimide and epoxy adhesives in flip chip packages can lead to crack propagation, interfacial moisture diffusion, and corrosion of metallized interconnections [2–4]. Although polyimides typically have poor adhesion to epoxy, they are widely used as chip passivation layers and organic substrates in microelectronic packaging due to their excellent chemical resistance, high glass transition temperature, high tensile strength, and low dielectric constant [1].

Plasma treatment of polymer surfaces is commonly performed to increase the adhesion strength of the polymer to other materials

[5]. Although plasma treatment typically improves the adhesion strength at polymer/polymer and polymer/metal interfaces, the mechanisms by which the adhesion is improved are not well understood [5]. Interfacial adhesion properties and mechanisms are dependent on the molecular structure of buried interfaces [5,6]. However, non-destructive *in situ* characterization of such buried polymer interfaces is challenging using conventional surface analytical techniques. Consequently, structure–property relationships at buried polymer interfaces are not well understood.

Among the many surface analytical techniques used to characterize polymer interfaces, sum frequency generation (SFG) vibrational spectroscopy has recently been utilized to non-destructively characterize molecular structures at buried polymer interfaces *in situ* [6–8]. SFG has recently been applied to correlate molecular structures at buried polymer interfaces to interfacial properties such as adhesion, interfacial water transport, and interfacial interaction energy [9–18]. In this paper, we utilized infrared-visible SFG vibrational spectroscopy to study the effects of polyimide plasma treatment on the molecular structure at buried polyimide/epoxy interfaces. The molecular structure of a polyimide surface was first characterized in air and then at the buried polyimide/epoxy interface. The effect of polyimide surface plasma treatment was studied by exposing the polyimide surface to

* Corresponding author.

E-mail address: zhanc@umich.edu (Z. Chen).

plasma prior to forming the polyimide/epoxy interface. The molecular structure at the plasma treated polyimide/epoxy interface was then compared to the molecular structure at the untreated polyimide/epoxy interface to deduce the molecular level effects of the plasma treatment. Analysis of SFG spectra collected in different polarization combinations enabled the possible tilt and twist angles of the polyimide backbone at the buried polyimide/epoxy interface to be determined before and after plasma treatment of the polyimide surface.

2. Experimental

2.1. Materials

N-Methyl-2-pyrrolidone (NMP), bisphenol A diglycidyl ether, and 4,4'-diaminodiphenylmethane were purchased from Sigma-Aldrich. Poly(pyromellitic dianhydride-co-4,4'-oxydianiline) amic acid solution (polyamic acid) was purchased from Sigma-Aldrich as a ~13 wt% solution in solvent. Calcium fluoride (CaF_2) right-angle prisms were ordered from Altos Photonics, Inc. and CaF_2 windows were ordered from ESCO Products, Inc.

2.2. Sample preparation

Poly(pyromellitic dianhydride-co-4,4'-oxydianiline) solution was diluted 1:3 by weight in NMP. Polyimide thin films were deposited by spin casting (Speedline Technologies P-6000) the diluted poly(pyromellitic dianhydride-co-4,4'-oxydianiline) solution on CaF_2 prisms or CaF_2 windows at 3000 RPM for 30 s. Cross-linked polyimide films were prepared by curing the poly(pyromellitic dianhydride-co-4,4'-oxydianiline) film in a vacuum furnace (STT-1200C-6-12 High Temperature Tube Furnace, Sentro Tech Corp.) at 260 °C for 60 min. The thickness of the cured polyimide films was ~50 nm based on profilometry measurements (DekTak 6 Profilometer). Epoxy precursor blends were prepared by mixing a stoichiometric ratio of bisphenol A diglycidyl ether and 4,4'-diaminodiphenylmethane. Polyimide/epoxy interfaces were prepared by depositing the epoxy precursor blend on the polyimide film followed by curing of the epoxy precursor blend for 1 h at 50 °C, 45 min at 75 °C, and 30 min at 110 °C [19]. Plasma treated interfaces were prepared by exposing cured polyimide films to oxygen or argon plasma for 10 s (Plasma Etch, Inc., PE-50), after which the plasma treated polyimide/epoxy interface was

prepared following the same procedure used to prepare untreated polyimide/epoxy interfaces.

2.3. Instrumentation

Fourier transform infrared vibrational spectroscopy: Infrared spectra were collected using a Thermo Scientific Nicolet 6700 Fourier transform infrared (FTIR) spectrometer. IR spectra were collected under a nitrogen atmosphere in the 1000–2000 cm^{-1} range with a resolution of 4 cm^{-1} from poly(pyromellitic dianhydride-co-4,4'-oxydianiline) thin films on CaF_2 windows. Prior to collection of the IR spectrum, the spin cast poly(pyromellitic dianhydride-co-4,4'-oxydianiline) thin film was cured at ~85 °C for 10 min to remove residual solvent. IR spectra were collected by averaging 32 scans before and after curing the poly(pyromellitic dianhydride-co-4,4'-oxydianiline) thin film to monitor the thermal imidization process.

Sum frequency generation vibrational spectroscopy: SFG has been extensively applied to study molecular structures at surfaces and buried interfaces [20–30]. SFG spectra were collected using a commercial SFG spectrometer purchased from EKSPLA, Inc. Details about the commercial SFG spectrometer can be found elsewhere [31]. SFG spectra were collected from polyimide/air and polyimide/epoxy interfaces of polyimide films on CaF_2 prisms by overlapping a fixed frequency 532 nm pulsed visible beam and a tunable pulsed infrared beam (2.3–10.0 μm) at the respective interface. The input angles of the visible and infrared beams were 60° and 54° at the sample stage, respectively, and the pulse energies of the input visible and infrared beams were ~20 μJ and ~100 μJ , respectively. SFG spectra were collected in the SSP (s-polarized SFG beam, s-polarized visible beam, p-polarized infrared beam) and PPP polarization combinations at ambient temperature and humidity (~20 °C and 40% relative humidity, respectively).

3. Results and discussion

3.1. Polyimide imidization

The curing of the poly(pyromellitic dianhydride-co-4,4'-oxydianiline) thin film (Fig. 1a) was monitored by collecting IR spectra of the film before and after thermal curing (Fig. 1b). IR spectra collected from the uncured film contained peaks near 1230, 1408, 1500, 1540, 1654, and 1726 cm^{-1} . Peaks near 1409, 1500, 1538,

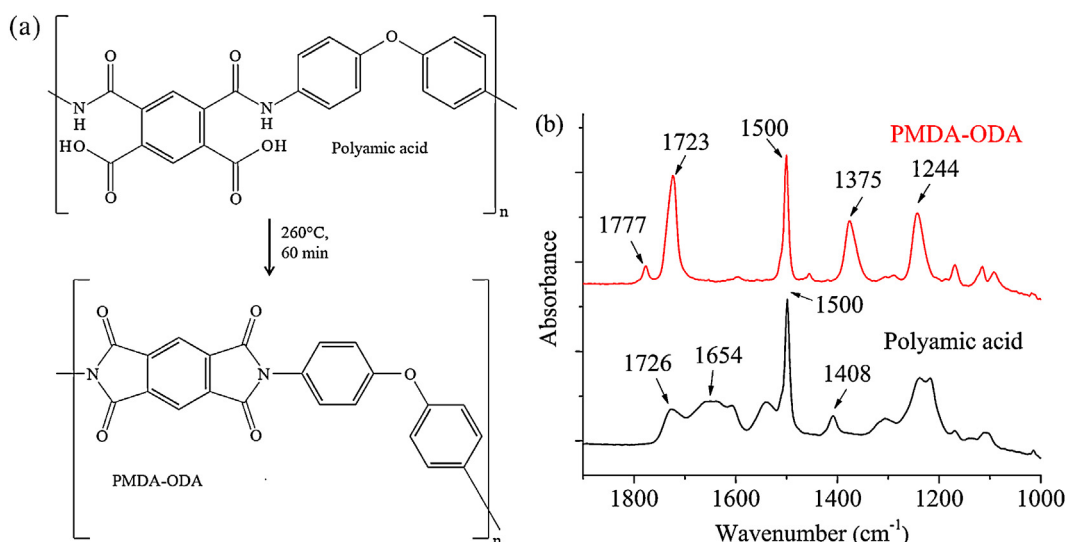


Fig. 1. (a) Polyamic acid cross-link reaction and (b) FTIR before (polyamic acid) and after (PMDA-ODA) thermal cure of polyamic acid. The FTIR spectra in (b) were offset vertically for clarity.

1654, and 1725 cm^{-1} can be assigned to the carboxylic acid –OH, the phenyl ring, –CNH amide II, C=O amide I, and carboxylic acid C=O stretches, respectively [32,33]. IR spectra collected from the cured film contained peaks near 1244, 1375, 1500, 1723, and 1777 cm^{-1} .

Peaks near 1244, 1375, 1500, 1723, and 1777 cm^{-1} can be assigned to COC, CNC, phenyl ring, imide I coupled C=O asymmetric, and imide I coupled C=O symmetric stretches, respectively [32,33]. The detection of a strong axial-imide II peak near 1375 cm^{-1} together with a lack of a carboxylic acid –OH feature near 1409 cm^{-1} in the IR spectrum collected from the cured film indicates that the imidization reaction was nearly complete after the thermal cure.

3.2. Polyimide/air and polyimide/epoxy interfaces

SFG spectra were collected in the 1650–1850 cm^{-1} range (of the input infrared beam) from the surface of cured polyimide films to characterize the molecular structure of the cured polyimide/air interface. Two peaks near 1733 and 1773 cm^{-1} were detected in the SFG SSP spectrum collected from the polyimide/air interface which can be assigned to the asymmetric (as) and symmetric (s) stretch of the coupled C=O groups on the imide ring (Fig. 2a) [34–37].

Strong SFG signal detected in the SSP polarization combination indicates that the infrared dipole moment of the detected vibrational mode had a dipole component perpendicular to the surface normal [38]. Therefore, based on the axis of infrared excitation of the asymmetric and symmetric vibrational modes shown in Fig. 2a, the symmetric peak in the SSP polarization combination will probe the tilt angle of the imide ring relative to the polyimide surface normal while the asymmetric peak will probe the twist angle of the coupled carbonyl groups in the plane of the imide backbone (Fig. S1 in Supporting information). The strong symmetric and weak asymmetric peaks observed in the SFG spectra collected from the polyimide/air interface suggest that the imide backbone was tilted from the surface normal and that the imide ring had a relatively high twist angle.

SFG spectra were then collected from the buried polyimide/epoxy interface to investigate how interactions between the epoxy and the polyimide influenced the polyimide molecular structure (Fig. 2b). Two peaks near 1735 and 1773 cm^{-1} were detected in the SFG SSP spectrum collected from the buried polyimide/epoxy interface, similar to the spectrum collected from the polyimide/air interface. However, the intensity of the asymmetric peak was much larger than the intensity of the symmetric peak. The high asymmetric to symmetric peak intensity ratio indicates that that

imide backbone was lying nearly parallel to the polyimide/epoxy interface and that the carbonyl groups were oriented with a low twist angle. Carbonyl groups oriented with a low twist angle indicate that one of the carbonyl groups on the imide chain was directed toward the epoxy bulk, different from the behavior at the polyimide/air interface where the carbonyl groups were oriented more parallel to the polyimide surface.

Different SFG spectra at the polyimide/air and polyimide/epoxy interfaces indicate that the molecular structure at the two interfaces was different. The strong asymmetric peak in the SFG spectra collected from the buried polyimide/epoxy interface suggests that the carbonyl groups on the imide backbone reoriented due to chemical interactions with the epoxy. Furthermore, the strong asymmetric peak suggests that the imide carbonyl group was oriented with a lower twist angle, i.e. the carbonyl was directed more toward the epoxy bulk, compared to the orientation at the polyimide/air interface. Polar interactions between the polyimide carbonyl and polar functional groups in the cross-linked epoxy may have caused the reorientation of the carbonyl group.

3.3. Polyimide plasma treatment

SFG spectra were first collected from the polyimide surface before and after plasma treatment to investigate whether ordered polyimide rings were present at the film surface after plasma treatment. The intensities of the peaks in the SFG SSP spectrum collected from the oxygen plasma treated polyimide/air interface were higher than at the original interface (Fig. 3a). In addition, more peaks were observed after the plasma treatment or the widths of the imide ring peaks increased. The higher signal intensities after oxygen plasma treatment could be due to new carbonyl groups generated by reactions between the polyimide surface and the oxygen plasma. Oxygen plasma treatment of polyimide has been reported to oxidize the imide rings and phenyl groups at the surface of the film [39–41]. Consequently, plasma treatment is commonly used to increase the surface hydrophilicity and surface energy of polyimide films [42]. Therefore, the additional carbonyl stretching signals observed after oxygen plasma treatment may have been contributed by carbonyl groups formed by oxidation of the imide ring or phenyl group by the oxygen plasma. Since this research is focused on the investigation of the buried polyimide interface using SFG as presented below, and plasma treatment of polyimide has been studied using other techniques [39–41], here we only characterized the polyimide surface after plasma treatment using SFG.

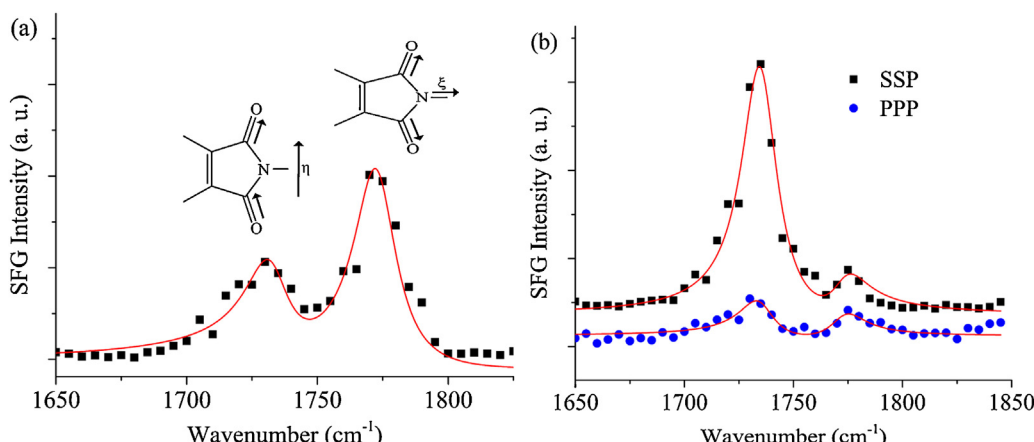


Fig. 2. SFG SSP spectrum collected from the (a) polyimide/air interface and SFG SSP and PPP spectra collected from the (b) buried polyimide/epoxy interface. The SFG spectra in (b) were offset vertically for clarity.

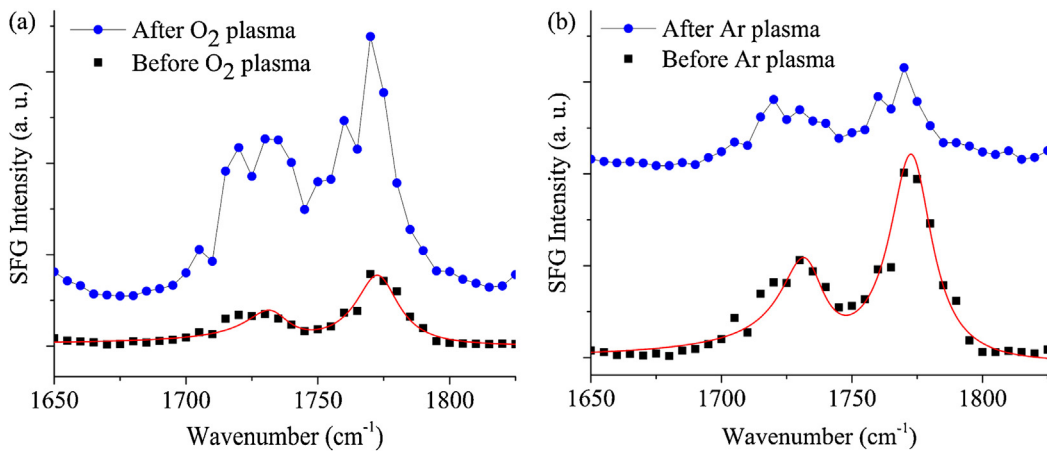


Fig. 3. SFG spectra collected from the polyimide/air interface before and after (a) oxygen and (b) argon plasma treatment. The SFG spectra in (a) and (b) were offset vertically for clarity. The solid red curves are the fitting results. The lines connecting the data points are a guide to the eye.

The spectral features of the SFG spectrum collected from the argon plasma treated polyimide/air interface (Fig. 3b) were similar to the features of the SFG spectrum collected from the untreated polyimide/air interface. Similar spectral features before and after plasma treatment indicate that the orientation of the polyimide rings at the polyimide/air interface was not largely affected by the plasma treatment. However, unlike the oxygen plasma treated polyimide/air interface, the intensities of the peaks in the spectrum collected from the argon plasma treated polyimide/air interface were lower than at the original interface. The decrease in the SFG intensity could be due to decreased ordering of the polyimide rings or to reactions between the ring and the argon plasma [41].

After characterizing the effects of plasma treatment on the molecular structure at the polyimide/air interface, SFG spectra were collected from buried polyimide/epoxy interfaces before and after plasma treatment of the polyimide film to characterize the effect of polyimide plasma treatment on the molecular structure of corresponding polyimide/epoxy interfaces. The SFG spectrum collected from the oxygen plasma treated polyimide/epoxy interface (Fig. 4a) was similar to the SFG spectra collected from the untreated polyimide/epoxy interface. However, the asymmetric to symmetric peak intensity ratio was lower than the intensity ratio at the untreated polyimide/epoxy interface which indicates that plasma treatment permanently altered the orientation of the imide backbone at the buried interface. The detection of SFG peaks contributed by imide ring vibrational modes at the plasma treated polyimide/epoxy interface indicates that ordered imide rings were present at the buried interface.

SFG SSP spectra collected from the argon plasma treated polyimide/epoxy interface (Fig. 4b) were similar to SFG spectra collected from the oxygen plasma treated polyimide/epoxy interface. The asymmetric to symmetric peak intensity ratio was again lower than the intensity ratio at the untreated polyimide/epoxy interface. To further characterize the effects of plasma treatment on the molecular structure at buried polyimide/epoxy interfaces, the possible orientations of the imide ring were determined before and after plasma treatment at the polyimide/air and polyimide/epoxy interfaces.

3.4. Orientation analysis

The orientation of the imide ring at the polyimide/air interface was estimated by assuming that the tilt angle was low ($\theta \approx 0\text{--}60^\circ$) based on the strong symmetric peak in the corresponding SFG spectrum. The experimentally determined $X_{yyz,\text{as}}/X_{yyz,\text{s}}$ value at the untreated polyimide/air interface was ~ 0.49 which indicates that the imide ring had a tilt angle in the range of $35\text{--}60^\circ$ and a twist angle in the range of $\sim 0^\circ$ to 42° (Fig. 5). The orientation of the imide ring was not estimated after oxygen and argon plasma treatment due to possible overlap between signals contributed by carbonyl groups and the imide ring.

We then assumed that the tilt angle of the imide ring at the buried polyimide/epoxy interface was almost parallel to polyimide surface ($\theta \approx 60\text{--}90^\circ$) based on the weak symmetric peak in the corresponding SFG spectrum. The $X_{yyz,\text{as}}/X_{yyz,\text{s}}$ ratio was not sensitive to changes in twist angle at high tilt angles (Fig. 6a), so the

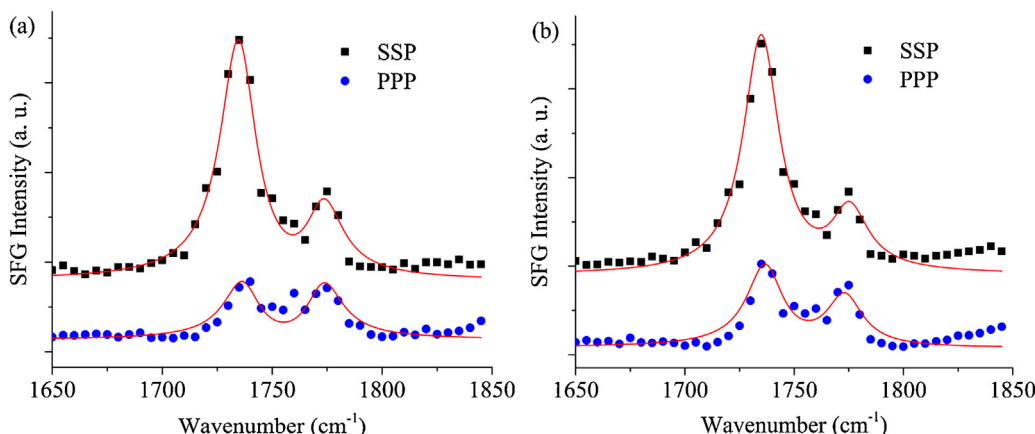


Fig. 4. SFG spectra collected from (a) oxygen and (b) argon plasma treated polyimide/epoxy interface. The SFG spectra in (a) and (b) were offset vertically for clarity.

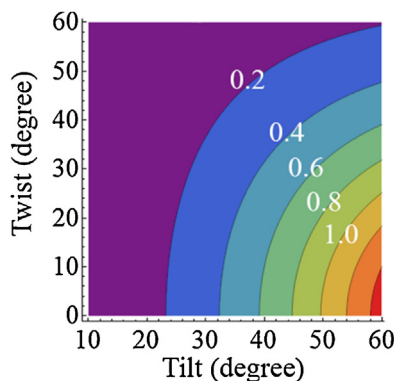


Fig. 5. Contour plot of $\chi_{yyz,as}/\chi_{yyz,s}$ as a function of tilt (θ) and twist (ψ) angles when the tilt angle is between 0 and 60°.

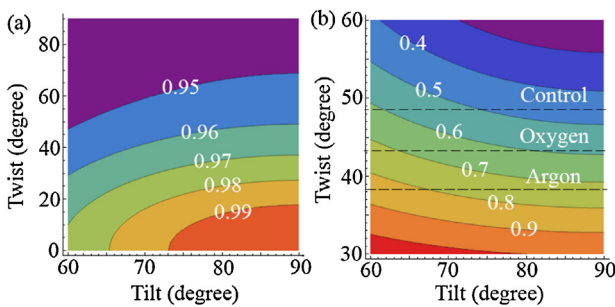


Fig. 6. Contour plots of (a) $\chi_{yyz,as}/\chi_{yyz,s}$ and (b) $\chi_{zzz,as}/\chi_{yyz,as}$ as a function of tilt (θ) and twist (ψ) angles when the tilt angle is between 60 and 90°.

$\chi_{zzz,as}/\chi_{yyz,as}$ ratio was used to determine the twist angle of the imide ring at the buried polyimide/epoxy interface. The experimentally determined $\chi_{zzz,as}/\chi_{yyz,as}$ value at the untreated polyimide/epoxy interface was ~0.47 which indicates that the imide ring had a twist angle of ~48° (Fig. 6b) at large tilt angles. After oxygen and argon plasma treatment, the imide ring twist angles at the buried polyimide/epoxy interface were ~43° and ~38°, respectively.

SFG orientation analysis suggests that plasma treatment resulted in a slight decrease in the twist angles of the imide ring at the buried polyimide/epoxy interface. The lower tilt angle of the imide ring after plasma treatment indicates that the carbonyl groups were directed slightly more into the epoxy bulk at the buried interface. If polymer chain scission occurred during the oxygen plasma treatment, entanglement loss could occur at the polyimide/air interface. Therefore, the different orientations of the imide ring at the polyimide/epoxy and plasma treated polyimide/epoxy interfaces may be due to greater flexibility of surface polyimide chains after plasma treatment.

4. Conclusion

In summary, we have demonstrated that plasma treatment of polyimide surfaces altered the molecular structure of corresponding polyimide/air and buried polyimide/epoxy interfaces. SFG results indicated that the polyimide backbone was tilted at the polyimide/air interface but was nearly lying down at the buried polyimide/epoxy interface. Furthermore, the twist angle of the imide backbone carbonyl groups at the buried polyimide/epoxy interface was slightly decreased after plasma treatment. Different molecular structures at the polyimide/air, polyimide/epoxy, and plasma treated polyimide/epoxy interfaces provide insight on the

molecular level effects of plasma treatment on adhesion strength and the lack of clear correlation between surface energy calculations and interfacial adhesion strength measurements [43]. More generally, these results indicate that plasma treatment of polymer surfaces not only increases the polymer surface energy, but can also influence the molecular structure at corresponding buried interfaces.

Acknowledgments

This work is supported by the Semiconductor Research Corporation (SRC contract No. 2012-KJ-2282). We thank Jaimal M. Williamson at Texas Instruments Inc., Dr. Kang-Wook Lee at IBM, and Dr. Chunyan Chen, Dr. Yuying Wei, and Dr. Yonghao Xiu at Intel Corporation for insightful discussions.

Appendix A. Supplementary data

Supplementary data associated with this article can be found, in the online version, at <http://dx.doi.org/10.1016/j.clet.2015.01.016>.

References

- V.K. Khanna, Adhesion-delamination phenomena at the surfaces and interfaces in microelectronics and MEMS structures and packaged devices, *J. Phys. Appl. Phys.* 44 (2011) 034004.
- S. Luo, C.P. Wong, Influence of temperature and humidity on adhesion of underfills for flip chip packaging, *IEEE Trans. Compon. Packag. Technol.* 28 (2005) 88–94.
- S.J. Luo, C.P. Wong, Effect of UV/ozone treatment on surface tension and adhesion in electronic packaging, *IEEE Trans. Compon. Packag. Technol.* 24 (2001) 43–49.
- P. Hoontrakul, L.H. Sperling, R.A. Pearson, Understanding the strength of epoxy-polyimide interfaces for flip-chip packages, *IEEE Trans. Device Mater. Reliab.* 3 (2003) 159–166.
- F. Awaja, M. Gilbert, G. Kelly, B. Fox, P.J. Pigram, Adhesion of polymers, *Prog. Polym. Sci.* 34 (2009) 948–968.
- Z. Chen, Investigating buried polymer interfaces using sum frequency generation vibrational spectroscopy, *Prog. Polym. Sci.* 35 (2010) 1376–1402.
- C. Zhang, J.N. Myers, Z. Chen, Elucidation of molecular structures at buried polymer interfaces and biological interfaces using sum frequency generation vibrational spectroscopy, *Soft Matter* 9 (2013) 4738–4761.
- J.M. Hankett, Y.W. Liu, X.X. Zhang, C. Zhang, Z. Chen, Molecular level studies of polymer behaviors at the water interface using sum frequency generation vibrational spectroscopy, *J. Polym. Sci. B: Polym. Phys.* 51 (2013) 311–328.
- K. Nanjundiah, P.Y. Hsu, A. Dhinojwala, Understanding rubber friction in the presence of water using sum-frequency generation spectroscopy, *J. Chem. Phys.* 130 (2009) 024702.
- C.L. Loch, D. Ahn, Z. Chen, Sum frequency generation vibrational spectroscopic studies on a silane adhesion-promoting mixture at a polymer interface, *J. Phys. Chem. B* 110 (2006) 914–918.
- C.L. Loch, D. Ahn, A.V. Vázquez, Z. Chen, Diffusion of one or more components of a silane adhesion-promoting mixture into poly(methyl methacrylate), *J. Colloid Interface Sci.* 308 (2007) 170–175.
- A.V. Vázquez, A.P. Boughton, N.E. Shephard, S.M. Rhodes, Z. Chen, Molecular structures of the buried interfaces between silicone elastomer and silane adhesion promoters probed by sum frequency generation vibrational spectroscopy and molecular dynamics simulations, *ACS Appl. Mater. Interfaces* 2 (2010) 96–103.
- C. Zhang, J.N. Myers, Z. Chen, Molecular behavior at buried epoxy/poly(ethylene terephthalate) interface, *Langmuir* 30 (2014) 12541–12550.
- C. Zhang, Z. Chen, Quantitative molecular level understanding of ethoxysilane at poly(dimethylsiloxane)/polymer interfaces, *Langmuir* 29 (2013) 610–619.
- J.N. Myers, C. Zhang, K.W. Lee, J. Williamson, Z. Chen, Hygrothermal aging effects on buried molecular structures at epoxy interfaces, *Langmuir* 30 (2014) 165–171.
- X. Zhang, J.N. Myers, J.D. Bielefeld, Q. Lin, Z. Chen, *In situ* observation of water behavior at the surface and buried interface of a low- K dielectric film, *ACS Appl. Mater. Interfaces* 6 (2014) 18951–18961.
- A. Kurian, S. Prasad, A. Dhinojwala, Direct measurement of acid–base interaction energy at solid interfaces, *Langmuir* 26 (2010) 17804–17807.
- Y. Fang, B.L. Li, J.C. Yu, et al., Probing surface and interfacial molecular structures of a rubbery adhesion promoter using sum frequency generation vibrational spectroscopy, *Surf. Sci.* 615 (2013) 26–32.
- S. Onard, I. Martin, J.-F. Chailan, A. Crespy, P. Carriere, Nanostructuration in thin epoxy–amine films inducing controlled specific phase etherification: effect on the glass transition temperatures, *Macromolecules* 44 (2011) 3485–3493.
- W.-T. Liu, Y.R. Shen, *In situ* sum-frequency vibrational spectroscopy of electrochemical interfaces with surface plasmon resonance, *Proc. Natl. Acad. Sci. U. S. A.* 111 (2014) 1293–1297.

- [21] J. Sung, G.A. Waychunas, Y.R. Shen, Surface-induced anisotropic orientations of interfacial ethanol molecules at air/sapphire (1̄02) and ethanol/sapphire (1̄02) interfaces, *J. Phys. Chem. Lett.* 2 (2011) 1831–1835.
- [22] C.M. Thompson, L.M. Carl, G.A. Somorjai, Sum frequency generation study of the interfacial layer in liquid-phase heterogeneously catalyzed oxidation of 2-propanol on platinum: effect of the concentrations of water and 2-propanol at the interface, *J. Phys. Chem. C* 117 (2013) 26077–26083.
- [23] H. Wang, A. Sapi, C.M. Thompson, et al., Dramatically different kinetics and mechanism at solid/liquid and solid/gas interfaces for catalytic isopropanol oxidation over size-controlled platinum nanoparticles, *J. Am. Chem. Soc.* 136 (2014) 10515–10520.
- [24] S.J. Ye, H.C. Li, W.L. Yang, Y. Luo, Accurate determination of interfacial protein secondary structure by combining interfacial-sensitive amide I and amide III spectral signals, *J. Am. Chem. Soc.* 136 (2014) 1206–1209.
- [25] F. Wei, H.C. Li, S.J. Ye, Specific ion interaction dominates over hydrophobic matching effects in peptide-lipid bilayer interactions: the case of short peptide, *J. Phys. Chem. C* 117 (2013) 26190–26196.
- [26] X.L. Lu, B.L. Li, P.Z. Zhu, G. Xue, D.W. Li, Illustrating consistency of different experimental approaches to probe the buried polymer/metal interface using sum frequency generation vibrational spectroscopy, *Soft Matter* 10 (2014) 5390–5397.
- [27] X.L. Lu, J.N. Myers, Z. Chen, Molecular ordering of phenyl groups at the buried polystyrene/metal interface, *Langmuir* 30 (2014) 9418–9422.
- [28] Q.F. Li, C.W. Kuo, Z. Yang, P.L. Chen, K.C. Chou, Surface-enhanced IR-visible sum frequency generation vibrational spectroscopy, *Phys. Chem. Chem. Phys.* 11 (2009) 3436–3442.
- [29] Q.F. Li, R. Hua, K.C. Chou, Electronic and conformational properties of the conjugated polymer MEH-PPV at a buried film/solid interface investigated by two-dimensional IR-visible sum frequency generation, *J. Phys. Chem. B* 112 (2008) 2315–2318.
- [30] J.N. Myers, C. Zhang, C.Y. Chen, Z. Chen, Influence of casting solvent on phenyl ordering at the surface of spin cast polymer thin films, *J. Colloid Interface Sci.* 423 (2014) 60–66.
- [31] J. Wang, C.Y. Chen, S.M. Buck, Z. Chen, Molecular chemical structure on poly(-methyl methacrylate) (PMMA) surface studied by sum frequency generation (SFG) vibrational spectroscopy, *J. Phys. Chem. B* 105 (2001) 12118–12125.
- [32] K. Ha, J.L. West, Studies on the photodegradation of polarized UV-exposed PMDA-ODA polyimide films, *J. Appl. Polym. Sci.* 86 (2002) 3072–3077.
- [33] W.S. Li, Z.X. Shen, J.Z. Zheng, S.H. Tang, FT-IR study of the imidization process of photosensitive polyimide PMDA/ODA, *Appl. Spectrosc.* 52 (1998) 985–989.
- [34] D. Kim, Y.R. Shen, Study of wet treatment of polyimide by sum-frequency vibrational spectroscopy, *Appl. Phys. Lett.* 74 (1999) 3314–3316.
- [35] D. Kim, M. Oh-E, Y.R. Shen, Rubbed polyimide surface studied by sum-frequency vibrational spectroscopy, *Macromolecules* 34 (2001) 9125–9129.
- [36] J. Sung, D. Kim, C.N. Whang, M. Oh-E, H. Yokoyama, Sum-frequency vibrational spectroscopic study of polyimide surfaces made by spin coating and ionized cluster beam deposition, *J. Phys. Chem. B* 108 (2004) 10991–10996.
- [37] M. Oh-E, H. Yokoyama, D. Kim, Mapping molecular conformation and orientation of polyimide surfaces for homeotropic liquid crystal alignment by nonlinear optical spectroscopy, *Phys. Rev. E* 69 (2004) 051705.
- [38] A.G. Lambert, P.B. Davies, D.J. Neivandt, Implementing the theory of sum frequency generation vibrational spectroscopy: a tutorial review, *Appl. Spectrosc. Rev.* 40 (2005) 103–145.
- [39] D. Wolany, T. Fladung, L. Duda, et al., Combined ToF-SIMS/XPS study of plasma modification and metallization of polyimide, *Surf. Interface Anal.* 27 (1999) 609–617.
- [40] S.H. Kim, S.W. Na, N.E. Lee, Y.W. Nam, Y.H. Kim, Effect of surface roughness on the adhesion properties of Cu/Cr films on polyimide substrate treated by inductively coupled oxygen plasma, *Surf. Coat. Technol.* 200 (2005) 2072–2079.
- [41] Y.S. Lin, H.M. Liu, H.T. Chen, Surface modification of polyimide films by argon plasma for copper metallization on microelectronic flex substrates, *J. Appl. Polym. Sci.* 99 (2006) 744–755.
- [42] K.W. Lee, S.P. Kowalczyk, J.M. Shaw, Surface modification of PMDA-oxydianiline polyimide. Surface structure–adhesion relationship, *Macromolecules* 23 (1990) 2097–2100.
- [43] P. Hoontrakul, R.A. Pearson, Surface reactivity of polyimide and its effect on adhesion to epoxy, *J. Adhes. Sci. Technol.* 20 (2006) 1905–1928.